A 3D Stacked Step-Down Intergrated Power Module

Wenbo Liu, Yan-Fei Liu, *Fellow, IEEE*
Department of Electrical and Computer Engineering
Queen's University,
Kingston, Canada
liu.wenbo@queensu.ca, yanfei.liu@queensu.ca

Laili Wang and Doug Malcolm
Sumida Technologies Inc.
Kingston, Canada
laili_wang@us.sumida.com,
doug_malcolm@us.sumida.com

***Abstract*— this paper presents a 3D integrated power module design to effectively save footprint and improve thermal performance. The design reduces the footprint by 40% using a 3D structure in which the inductor is over the top of the regulator. A fixed inductor with a cavity is used to envelop the 3D power module, and the high thermal conductivity of the magnetic core significantly enhances heat dissipation. An efficiency-wise design is applied to the proposed power module and there is a reduction in inductor DC resistance, which can in turn further improve the thermal performance. An analytical thermal model is built to calculate the temperature, 3D FEA (Finite Element Analysis) simulation is also utilized to estimate the improvement in temperature field. A prototype is built to test the electrical and thermal performances as well. The DCR is reduced by more than 30% and the thermal performance is improved by 8-10°C compared with plastic molded power modules.**

Keywords—3D power module; intergrated inductor; thermal analysis; FEA simulation

I. INTRODUCTION

Integrated power modules featuring high power density, high efficiency, high switching frequency and low cost are widely desired [1]. They are frequently used in applications like computers, telecommunication, uninterruptible power supply (UPS), electrical vehicles (EV), wind turbine and photovoltaic (PV) systems.[2][3] Step-down Buck power modules shown in Fig. 1 have become one of the major products of the modules in recent years, especially in computing, FPGA, network servers and telecom electronics [4]. However, as the requirement of power density keeps growing, it is quite challenging to use conventional two dimension wire bonding or planar structures to make continued improvements [5]. Also, bulky magnetic components in power converters always impose restrictions on reduction of the total size [6][6]. Thus, novel structures should be proposed to accommodate the requirement of higher power density.

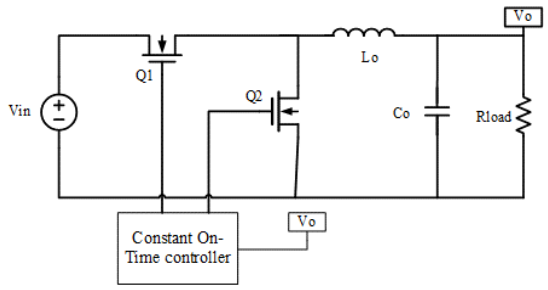

Fig. 1. Step-down Converter Circuit

Going vertical and using 3D packaging technology is one method that can highly improve the power density. It integrates the whole power module into z-axis layers and implements a smaller footprint [7]. Several methods with the purposed of analyzing the thermal performance of 3D power modules have been proposed [13], [9]. However, the thermal performance of 3D products is always severely limited by several obstacles. Firstly, high power density imposes a big challenge: larger power capacity means more heat is generated and the highly compacted downsized package blocks the convection outwards. Secondly, the multi-layer structure has poor ability to dissipate heat from the upper layer to the PCB so that the upper devices are easily to be heated up. Usually for an electronic system, the lifetime obeys the "10°C—twice law" (lifetime becomes half if the operating temperature is 10°C increased) and the failure rate will increase 10—30 times if it is 20°C hotter [10].Therefore, decreasing the junction temperature of IC is a very important design objective which improves not only the performance but the reliability [11-13]. Especially for 3D power modules, an effective solution is required to properly settle the cooling problem.

In this paper, a 3D structure power module based on power supply in inductor (PSI^2) technology is presented. This technology is a kind of magnetic integration which explores a fixed inductor on the top of the PCB and it also serves as the case of the whole module instead of plastic molding. The magnetic and thermal analyses of power supply in inductor (PSI^2) are presented in [14], [15]. The proposed structure combines the advantages of 3D packaging and magnetic integration: firstly, the 3D structure utilizes the space more efficiently, increasing the power density; secondly, the heat dissipation is enhanced due to the high thermal conductivity of magnetic material. Also, magnetic integration allows an improved inductor design to reduce the direct current resistance (DCR) and decrease the loss. The paper is organized as below: Section II describes principle of the 3D power module, Section III presents the inductor design, loss analysis and electromagnetic analysis

using FEA (Finite Element Analysis), Section IV uses ANSYS FEA simulation to predict the thermal performance. Section V demonstrates the experimental results of the proposed prototype. Section VI concludes the paper.

II. Principle of 3D Packaging Structure and Fabrication Process

An isometric drawing of the proposed 3D integrated power module is shown in 0 to illustrate the idea of the structure. The power supply in inductor (PSI^2) technology is used to make integrated power modules without plastic molding, in this kind of structure the inductor also serves as the case of the module. The regulator (controller and 2 MOSFETs) and auxiliary components are mounted on the PCB (print circuit board), and a coil is attached to the PCB through 2 vertical leads. Fig. 3 shows the configuration of a plastic molded power module as a comparison. The inductor, regulator and auxiliary components distribute on the substrate and the total module is molded with epoxy plastic

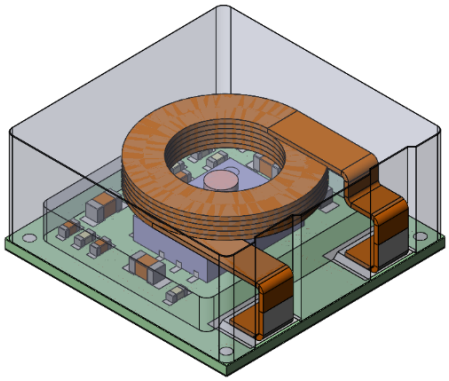

Fig. 2. Isometric View of the Proposed Power Module

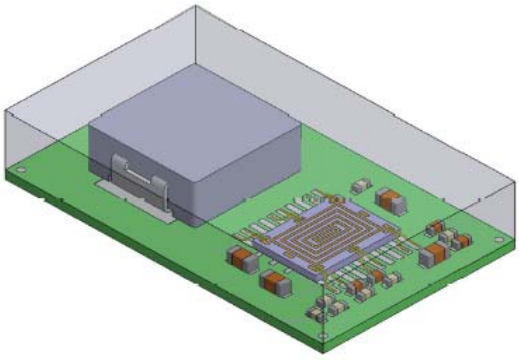

Fig. 3. Traditional 2D Plastic Packaged Power Module

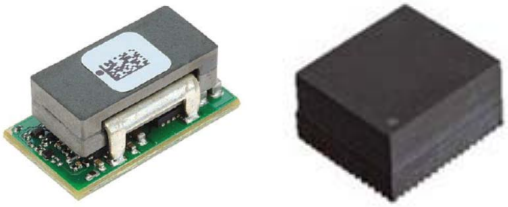

Fig. 4. 3D Power Modules: (a)Open Frame (b)Plastic Molded

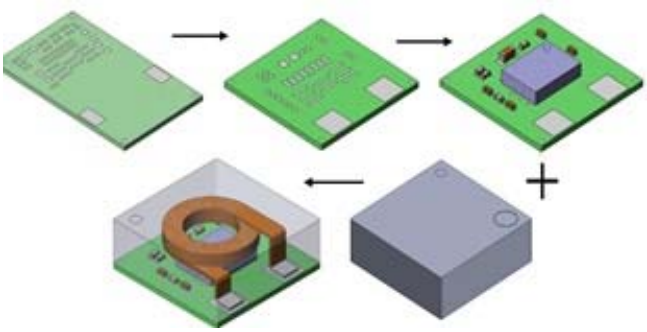

Fig. 5. Fabrication Process of 3D Power Module

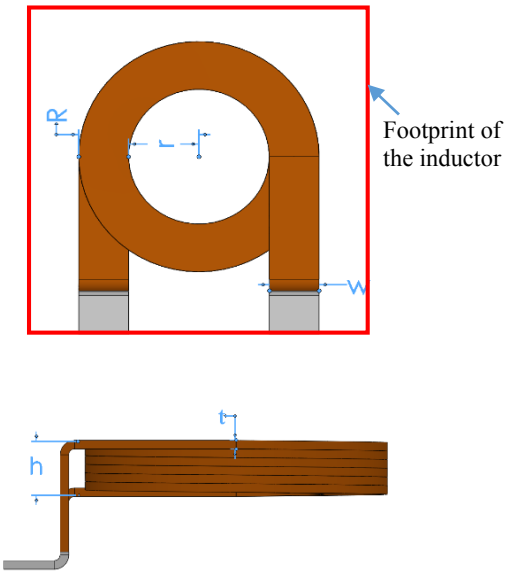

Fig. 6. Dimensions of the Winding (a) Top View (b) Side View

material. It is noted that each of the devices of the 2D power module occupies area on the substrate, and the inductor takes up the most area. By contrast, in the 3D structure, the inductor winding is over the top of the other components, allowing the PCB area to be reduced by 40% in comparison to the conventional design. In this principle, the size of a step-down power module is reduced to 9mm by 9mm from 15mm by 9mm. Conventional 3D open frame power module and integrated plastic molded 3D power module are shown in Fig. 4 as comparisons. Fig. 5

Also, in the conventional power module, the inductor size is limited by the plastic mold (smaller than the mold to leave enough room). But in the proposed 3D stacked structure there is no plastic casing, so the inductor footprint can be expanded to the same as total power module footprint. Therefore the inductor size can still be larger although the total PCB area is reduced. Thus larger effective core area and more coil number of turns can be utilized, allowing an improved inductor design. So the proposed power module can obtain smaller winging direct current resistance (DCR)

without losing inductance. The wise efficiency design will be discussed in the next section.

Figure 5 introduces the fabrication process of the proposed power module. The inductor is moved to the top of IC, its solder pads are relocated on board close to the regulator. Then the regulator and the auxiliary resistors and capacitors are mounted on the PCB. Afterwards the inductor is mounted and it covers the components. Finally, the total fabrication process is completed and an integrated 3D stacked power module is obtained. The selection of inductor will be discussed in the third section.

III. Inductor Design and Analysis

This section will discuss the inductor design process and the impact of inductor footprint and the profile (height). Magnetic parameters and losses are analyzed to support the design. FEA simulation is applied to verify the analysis and predict the electrical and magnetic performances.

Initial calculation based on the mechanical properties of the inductor are performed to give a predesign. For the proposed power module prototype, the specification of this step-down Buck converter is set as 9-15V input, 0.6-5V output with 6A full-load, and the operating frequency is 800 kHz. The current ripple is determined by (1),

$$I_{p-p} = \frac{(V_{in}-V_{out})\cdot D}{L\cdot f_s} = \frac{V_{in}D(1-D)}{L\cdot f_s} \qquad (1)$$

According to this formula, the largest current ripple occurs at 5V output the required inductance is 1.1uH. For an inductor with a coil shaped with flat wire as shown in Fig. 6, the inductance is calculated by (2)-(4).

$$L = \frac{\mu_r \mu_0 N^2 A_e}{l} \qquad (2)$$

$$l = 2h + 2w + r \qquad (3)$$

$$A_e = \pi \cdot r^2 \qquad (4)$$

Where h is the height of the winding, w is the wire width, A_e is the flux effective area, r is the inner radius and l_e is the length of flux path. The designators are marked in Fig. 6, and the red border presents the inductor footprint [16-18].

Benefiting from the flexibility of the power supply in inductor (PSI^2) as described in section II, the proposed power module allows a larger inductor footprint. This design focuses on minimizing the winding resistance without decreasing the inductance. By sweeping the value of inductor footprint, the number of winding turns are obtained. Table I shows the calculated required wire coil number of turns and their justified results for 1.1uH inductance. Conditions when the required inductance is 0.7uH and 1.5uH are also investigated. The trend curves of number of turns at different footprint and inductance are shown in Fig. 7. Half of the turns can be saved when the inductor footprint increases from 5mm to 9mm.

TABLE I. Required Number of Turns vs Footprint (L=1.1uH)

Footprint (mm^2)	Number of turns	Justified turns N	DCR(mΩ) (2.4mm of total height)
5^2	8.14	8.25	18.7
5.5^2	7.40	7.5	15.5
6^2	6.78	6.75	12.5
6.5^2	6.26	6.25	10.7
7^2	5.81	5.75	9.1
7.5^2	5.42	5.5	8.3
8^2	5.08	5	6.9
8.5^2	4.79	4.75	6.2
9^2	4.52	4.5	5.6

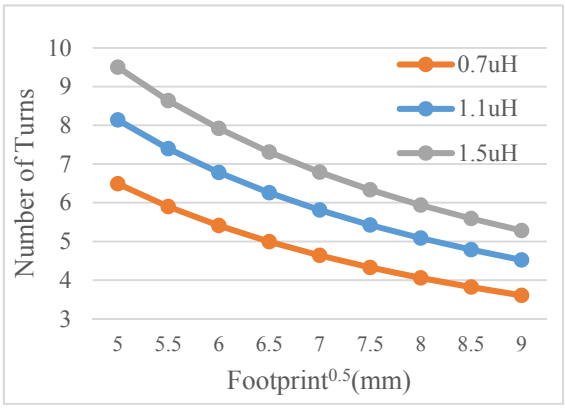

Fig. 7. Required Number of Turns vs Inductor Footprint

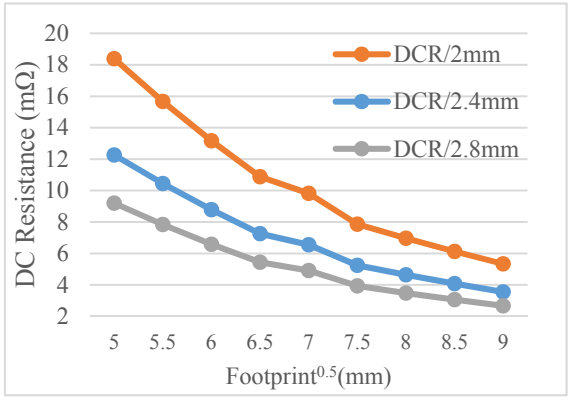

Fig. 8. Calculated DCR vs Inductor Footprint (0.7uH)

Besides the footprint, height is always another critical restriction for the power modules (especially 3D power modules). Accomplishing the design requirement with a low profile is another goal of this design. Assume the height of inductor is fixed, then coils with more number of turns have to use thinner wire to keep in the same profile so that the DCR becomes fairly large. Fig 8-10 show the calculated

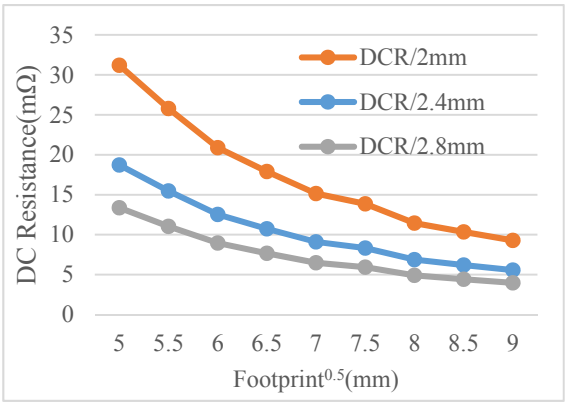

Fig. 9. Calculated DCR vs Inductor Footprint (1.1uH)

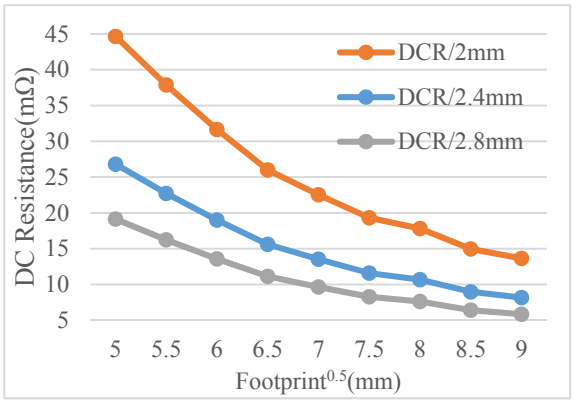

Fig. 10. Calculated DCR vs Inductor Footprint (1.5uH)

DCR at different inductor footprint and height. The DCR can be calculated by parameters in Fig. 6 with (5).

$$R_{dc} = \rho_w \frac{2\pi N(r+\frac{w}{2})}{t \cdot w} \quad (5)$$

For each required inductance, winding configurations with the height of 2mm, 2.4mm and 2.8mm are analyzed to estimate their winding resistances. It can be concluded from the figures that for a given height, the inductor with a larger footprint has less turns and smaller DCR; and for a given footprint, the higher the profile, the smaller the DCR. Basically less turns of wire allows utilization of thicker wire; and higher profile also means that the wire is thicker. Therefore the results do match the common sense.

However, higher inductor has longer magnetic path length, which in turn reduces the inductance. Moreover, high profile is always not ideal for any power modules. In consequence, a proper thickness of wire instead of has thick as possible is preferred. In order to reduce the DCR and avoid extremely high profile, a configuration with 4.75 turns coil formed by 0.25mm thick flat wire is selected. For the other parameters w is 1.2mm, r=2mm. The actual inductance is 1.05μH and DCR is 6.8mΩ which match the pre-calculation result well. The total height of the module is 4.0mm, including a 2.4mm inductor, a 1.2mm regulator and a 0.4mm substrate. Further electromagnetic and thermal analysis will be performed based on the selected configuration.

A series of Maxwell FEA simulation was proposed to analyze the impact of how the height is arranged. The thickness of magnetic material above and beneath the coil is assumed to be the same. Table II shows the height of power module at different winding and core height. Table III shows how much thickness of magnetic material affects the inductance of a 4.75 turns winding inductor. It can be observed that the inductance increases slightly with the total height of the module, but the DCR changes a lot with the wire thickness. So thicker wire draws more benefit for inductor design than thicker magnetic material. For instance, the height of the configuration with 0.25mm flat wire and 0.6mm core material above and beneath the coil is the same as that of the inductor utilizing a 0.16mm wire and 0.9mm magnetic material. The inductance of the second inductor (1.26uH) is 25% higher than the first (0.99uH). Meanwhile, DCR is increased by 65% (9.3mΩ compared with 5.6mΩ). In conclusion, a further modified design with much smaller DCR and enough inductance can be achieved by using less magnetic material and thicker wire.

A prototype of the chosen layout was built and experiment was conducted. With DC bias from 0A to 8A, it can be confirmed that the inductance is no smaller than 900nH, which still satisfies the requirement of Buck converter with higher load current. As a result of magnetic simulation, the maximum flux density of B is 0.280T at 6A

TABLE II. TOTAL HEIGHT WITH DIFFERENT WIRE AND CORE

Magnetic material (mm) / Wire(mm)	0.60	0.65	0.70	0.75	0.80	0.85	0.90
0.16	3.42	3.52	3.62	3.72	3.82	3.92	4.02
0.19	3.61	3.71	3.81	3.91	4.01	4.11	4.21
0.22	3.81	3.91	4.01	4.11	4.21	4.31	4.41
0.25	4.00	4.10	4.20	4.30	4.40	4.50	4.60
0.28	4.20	4.30	4.40	4.50	4.60	4.70	4.80
0.31	4.39	4.49	4.59	4.69	4.79	4.89	4.99
0.34	4.59	4.69	4.79	4.89	4.99	5.09	5.19

TABLE III. INDUCTANCE WITH DIFFERENT WIRE AND CORE

Magnetic material (mm) / Wire(mm)	0.60	0.65	0.70	0.75	0.80	0.85	0.90
0.16	1.16	1.18	1.20	1.21	1.23	1.25	1.26
0.19	1.09	1.11	1.13	1.14	1.16	1.17	1.19
0.22	1.04	1.06	1.07	1.09	1.10	1.11	1.12
0.25	0.99	1.01	1.02	1.03	1.05	1.06	1.07
0.28	0.95	0.96	0.97	0.99	1.00	1.01	1.02
0.31	0.91	0.93	0.94	0.95	0.96	0.97	0.98
0.34	0.88	0.89	0.90	0.91	0.92	0.93	0.94

full load, which is still far from saturation (start from 0.35T for the selected material as well as most of the magnetic material).

IV. Thermal Analysis and FEA Simulation

This section presents thermal analysis of the proposed power module with the help of equivalent circuit thermal model and FEA simulation. The thermal resistance of each part is calculated and comparisons are made to observe how much the cooling performance is enhanced by power supply in inductor (PSI^2).

Junction to ambient thermal resistance is an important parameter for power electronic products. Usually, smaller thermal resistance results in lower temperature rise. In still air convection mode, the temperature rise at steady-state is related to total dissipated power and thermal resistance as (6)-(9):

$$\Delta T = q * R_{total} \quad (6)$$

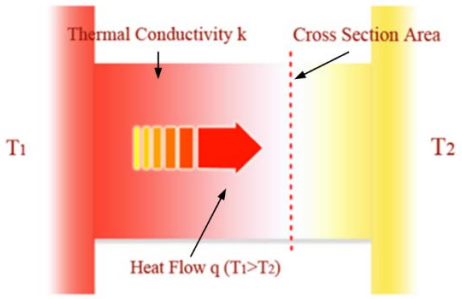

Fig. 11. Distribution of Heat Sources in 3D Power Module

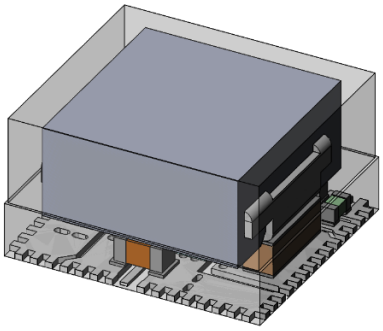

Fig. 12. CAD Drawing of Plastic Molded 3D Power Module

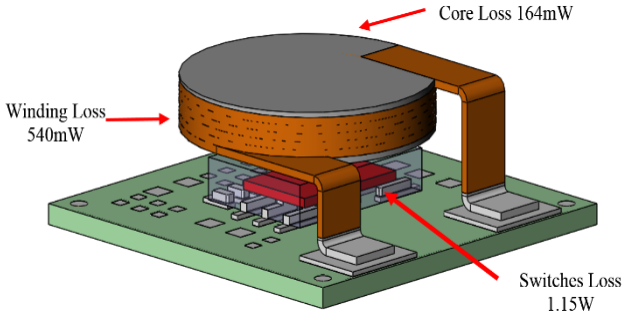

Fig. 13. Distribution of Heat Sources in 3D Power Module

$$R_{total} = R_{convection} + R_{conduction} \quad (7)$$

$$R_{conduction} = g * \frac{d}{k*A} \quad (8) \qquad R_{convection} = \frac{1}{h*A} \quad (9)$$

Where q is the power of heat dissipation, d is the length of material, g is the geometry factor, k is the thermal conductivity, A is the contact area of the objects and h is the thermal coefficient of air. The designators are shown in Fig.11, T_1 is the high temperature and T_2 is the ambient. The integrated power module utilizes a high thermal conductivity to reduce the thermal resistance and enhances the heat dissipation.

FEA simulation is applied to estimate the thermal performance of the proposed structure, in comparison with a plastic molded 3D power module. Fig. 12 illustrates a CAD drawing of the plastic module which uses very thick wire to achieve small DCR. Its profile is very high as a result (8.5mm by 7.5mm by 4.7mm). The operating condition for both modules is 12V input, 5V output with 6A load current. The loss of proposed converter is estimated and divided into 3 major parts: winding loss (540mW from I^2R calculation), core loss (164mW from MAXWELL simulation) and regulator loss (switches loss, gate drive loss and other quiescent losses, rest of the total loss, 1.15W). Fig. 13 shows the idea of loss breakdown and their distribution.

FEA simulation was utilized to estimate the thermal performance of the proposed power module. Utilizing computer assist design software like Solidworks, mechanical models featuring high accuracy are obtained. The models are imported into ANSYS workbench and thermal simulations are executed. The simulation results can illustrate temperature of each individual element of the models. In the

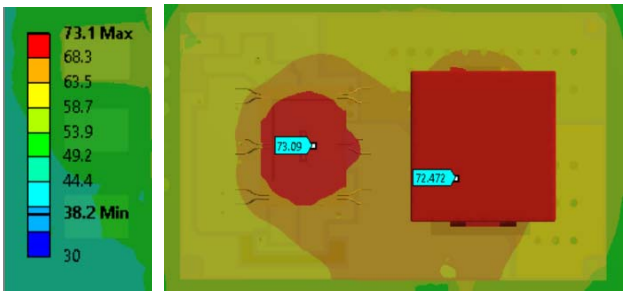

Fig. 14. 2D Plastic Module with 750mW Winding Loss, 2.1W Total Loss

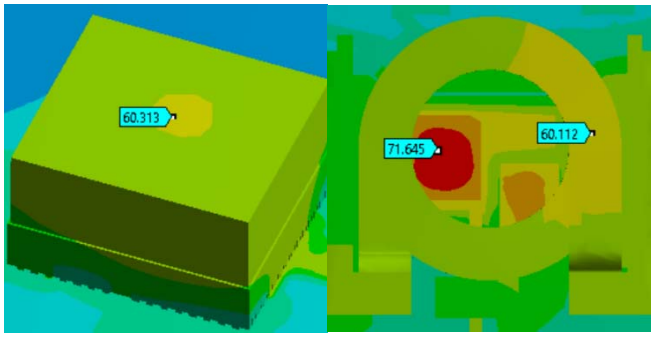

Fig. 15. Simulation Results for the 3D Plastic Power Module

TABLE IV. SIMULATION RESULTS VERSUS VARIOUS THERMAL CONDUCTIVITIES

Thermal conductivity(W/K.m)	Open frame	0.5	0.75	1	1.5	2	3
Case temp(°C)	67.2	64.9	67.6	62.6	62.0	61.4	58.9
Regulator(°C)	89.6	74.7	70.5	67.7	71.4	68.7	62.2

simulation models of this paper, the power modules are mounted on 60mm×80mm host PCBs (named as thermal boards) and operate with full load condition (5Vout/6A load). The ambient is still air and the temperature is 22°C. Comparisons were made based on the simulation results to analyze the impact of factors such as structure and properties of material.

Fig. 14 and 15 show the steady-state thermal simulation results for conventional plastic molded power modules. In Fig. 14, temperature of a 2D power module is presented. Its footprint is 15mm*9mm and footprint of the inductor is 5.5mm*5.5mm. The winding resistance is 15.6mΩ and the winding loss is 750mW according to I^2R calculation (6A current). The maximum temperature which corresponds the junction is 72°C and the top case maximum temperature is 60°C. Fig. 15 shows the simulation result of a 3D plastic power module with a high profile inductor. It features small DCR (11mΩ) and high efficiency (94.5% at full load, winding loss is 500mW). Thus the conventional integrated power modules have poor thermal performance and the 3D structure is even worse with the same power loss.

Fig. 16 presents the thermal simulation result for the proposed 3D power module. Fig. 16(a) is an estimation for a power module with the same loss as the 3D plastic molded power module. Its junction temperature is 62.2°C and the case temperature is 58.9°C. Fig. 16(b) presents the result for the proposed power module prototype with a 4.4mm high profile, whose loss is only 1.7W. Its junction temperature is 58°C and the case temperature is 53.6°C.

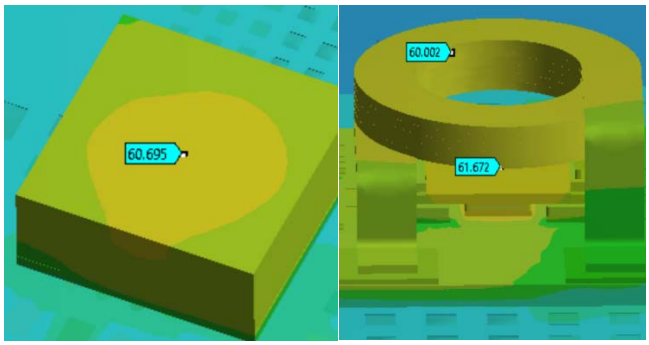

(a) 500mW Copper Loss, 1.85W Total Loss

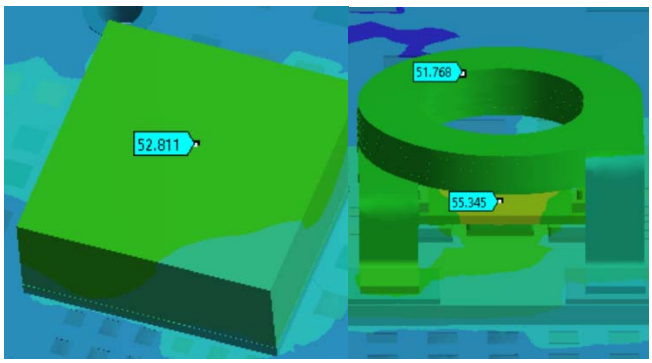

(b) 350mΩ Copper Loass, 1.7W Total Loss

Fig. 16. Simulation Results for the Proposed 3D Power Module

To conclude from the simulation results, the proposed 3D integrated power module would have an 8°C lower junction temperature rise than the 3D plastic power module with the same loss according to Fig. 15 and Fig. 16 (a). This improvement can rise to more than 15°C after further modification of the inductor, which is quite significant.

Several simulations in FEA were performed for the proposed 3D module using varying values of thermal conductivity for the case. The loss is assumed to be 1.85W in these simulations. It can be conclude from Table IV that thermal conductivity affects the temperature rise. The difference between a thermal conductivity of 0.75W/K.m and 3W/K.m is around 8.3°C in the simulation although the case top temperature does not change much. According to this simulation, the material in which the heat transfers plays a critical role in the temperature rise. This indicates how the junction temperature is reduced in the proposed 3D power module.

V. PROTOTYPE AND TEST

A prototype of the proposed 3D integrated power module is built to test its performances in comparison with other two plastic molded power modules. The three modules have same input and output specifications and they are soldered on the same test boards.

The actual size of prototype is 8.8mm×8.5mm×4.1mm, with a 4.75 turns winding formed by 1.2mm×0.25mm flat copper wire. Fig. 17 illustrates the top view of the proposed 3D power module and the picture of test board which is a 4 layer board with a size of 60mm*80mm. Product #1 is a conventional 2D power module with 15mm×9mm×2.8mm footprint. Product #2 is a 3D plastic power module with a high profile inductor and its size is 8.5mm×7.5mm×4.7mm. Specification of all the products is 12V input, 5V output with 6A maximum load current. Product #1 and #2 are also mounted on the same PCBs as the proposed module to make comparisons.

Fig. 18 shows the efficiency curves of the three power modules. Benefiting from the larger footprint and slightly higher profile of inductor, the winding resistance of proposed 3D power module is smaller than that of product #1 so that it has a higher efficiency. The peak efficiency is 95.4% at half load and full load efficiency is 94.7%.

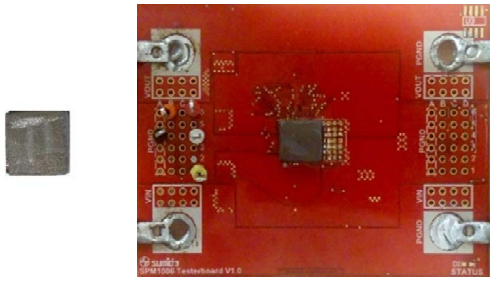

Fig. 17. Top View of the Proposed 3D Power Module

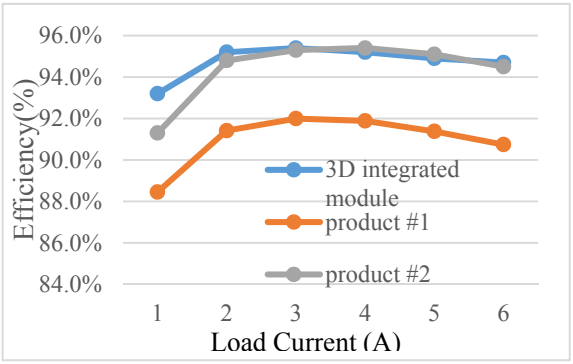

Fig. 18. Efficiency Curves of the Power Modules

Product #2 utilizes a very high profile inductor so that it also allows a small DCR and achieves high efficiency (94.5% at full load).

Meanwhile, IR camera is utilized to validate the thermal performance of the power modules. Fig. 19 shows the thermal image of the integrated 3D module at 5Vout/6A load in steady state, and the maximum top case temperature is 59.2°C and its regulator is 63°C according to the thermocouple measurement. The total loss is 1.75W in this case and the efficiency is 94.7%. Fig. 20 shows the thermal image of the 2D plastic molded power module at the same load, its total loss is 2.4W and the maximum case temperature 71.2°C. Fig. 21 presents the performance of 3D plastic module (product #2), the loss is 1.78W in this load condition and the top case temperature is 60.1°. The proposed power module achieves a lower top case temperature than the 3D plastic module.

As the thermal conductivity of core material is much better than plastic, the difference of junction temperature is larger. Based on the definition of junction to case thermal resistance, the junction temperature can be approximately calculated by (10) [22].

$$\theta_{JC} = (T_J - T_C)/P_H$$

θ_{JC} of product #2 is 5.7~6.7K/W according to the datasheet, and the measured power of heat is 1.78W. So the maximum junction temperature is around 71°C, which also matches the simulation result closely. Thus the proposed integrated power module can achieve 7-10°C better thermal performance than the high efficiency 3D plastic molded power module, and it proves that power supply in inductor (PSI^2) is a good solution to the cooling problem of 3D structure.

VI. Conclusion

A novel 3D integrated power module featuring high efficiency, improved thermal performance and smaller footprint is proposed in this paper. This power module combines the advantages of 3D structure and novel packaging technology, its footprint can be reduced by 40% and the inductor winding loss can be reduced by 30% compared to a traditional 2D structure. By utilizing power supply in inductor (PSI^2) technology, the thermal performance is significantly improve: junction temperature can be decreased 10°C without reducing efficiency compared to a plastic 3D structure. An FEA simulation is performed to optimize the inductor design and estimate the thermal performance, and a prototype was built to validate the simulation. Simulation and experimental results verify that improved electrical and thermal performances are achieved.

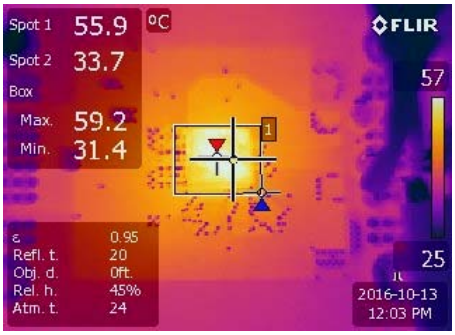

Fig. 19. Thermal Image of Integrated 3D Power Module

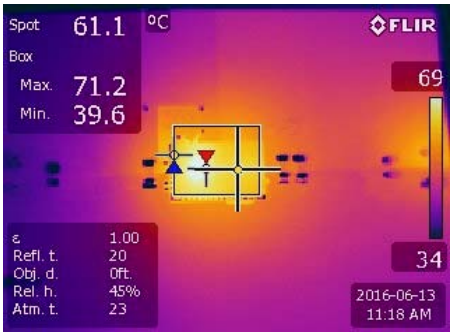

Fig. 20. Thermal Images of 2D Plastic Module

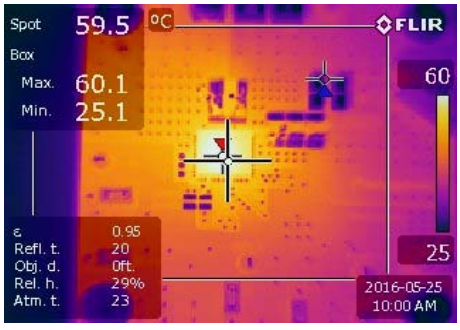

Fig. 21. Thermal Images of 3D Plastic Module

REFERENCES

[1] Ménager, L., Martin, C., Allard, B., & Bley, V. (2006, November). Industrial and lab-scale power module technologies: A review. In IEEE Industrial Electronics, IECON 2006-32nd Annual

[2] Liu, C. K., Chao, Y. L., Chang, J. C., Li, W., Tzeng, C. M., Fang, R. C., ... & Lo, W. C. (2012, December). IGBT power module packaging for EV applications. In *Electronic Materials and Packaging (EMAP), 2012 14th International Conference on* (pp. 1-4). IEEE.

[3] Skoplaki, E., & Palyvos, J. A. (2009). On the temperature dependence of photovoltaic module electrical performance: A review of efficiency/power correlations. *Solar energy*, *83*(5), 614-624.

[4] Matsumoto, K., Nishijima, K., Sato, T., & Nabeshima, T. (2011, May). A two-phase high step down coupled-inductor converter for next generation low voltage CPU. In *Power Electronics and ECCE Asia (ICPE & ECCE), 2011 IEEE 8th International Conference on* (pp. 2813-2818). IEEE.

[5] Liu, Y. O., & Kinzer, D. (2011, April). Challenges of power electronic packaging and modeling. In Thermal, Mechanical and Multi-Physics Simulation and Experiments in Microelectronics and Microsystems (EuroSimE), 2011 12th International Conference on (pp. 1-9). IEEE.

[6] Liu, Tianshu, et al. "A novel asymmetrical three-level BUCK (ATL BUCK) converter for point-of-load (POL) application." *Energy Conversion Congress and Exposition (ECCE), 2015* IEEE, 2015.

[7] Davis, W.R., Wilson, J., Mick, S., Xu, J., Hua, H., Mineo, C., Sule, A.M., Steer, M. and Franzon, P.D., 2005. Demystifying 3D ICs: the pros and cons of going vertical. *Design & Test of Computers, IEEE*, *22*(6), pp.498-510.

[8] Hirohata, K., Hisano, K., Mukai, M., Aoki, H., Takubo, C., Kawakami, T., & Pecht, M. G. (2010). Coupled thermal-stress analysis for FC-BGA packaging reliability design. *Components and Packaging Technologies, IEEE Transactions on*, *33*(2), 347-358.

[9] Yamada, Y., Yu, Q., Takahashi, T., & Takagi, Y. (2012, December). Study on thermal design due to downsizing of power module using coupled electrical-thermal-mechanical analysis. In *Electronic Materials and Packaging (EMAP), 2012 14th International Conference on* (pp. 1-7). IEEE.

[10] Apiste technical information: Panel cooling units, http://www.apiste-global.com/enc/technology_enc/detail/id=1262

[11] Takahashi, Tomohiro, and Q. Yu. "Precision evaluation for thermal fatigue life of power module using coupled electrical-thermal-mechanical analysis." *Electronics Packaging Technology Conference (EPTC), 2010 12th* IEEE, 2010:201-205.

[12] Wang, M. H., et al. "Thermal-moisture coupling effects on PA and UF war page stress of 2.5D IC package by FE simulation analysis. "*Microsystems, Packaging, Assembly and Circuits Technology Conference (IMPACT), 2014 9th International* IEEE, 2014:129-133.

[13] Lan, Jia Shen, and M. L. Wu. "An analytical model for thermal failure analysis of 3D IC packaging." *Thermal, mechanical and multi-physics simulation and experiments in microelectronics and microsystems (EuroSime)*, *2014 15th international conference on IEEE*, 2014:1-5.

[14] Laili Wang, W. Liu, D. Malcolm and Y-F. Liu. "Thermal Analysis of a Magnetic Packaged Power Module" *Applied Power Electronics Conference and Exposition, 2016. APEC 2016. Thirty-first Annual* IEEE, 2016.

[15] Laili Wang, D. Malcolm and Y-F. Liu. "An Innovative Power Module with Power-System-In-Inductor Structure" *Applied Power Electronics Conference and Exposition, 2016. APEC 2016. Thirty-first Annual* IEEE, 2016

[16] Wang, L., Hu, Z., Liu, Y. F., Pei, Y., Yang, X., & Wang, Z. (2013). A Horizontal-Winding Multipermeability LTCC Inductor for a Low-profile Hybrid DC/DC Converter. *Power Electronics, IEEE Transactions on*, *28*(9), 4365-4375.

[17] Wang, L., Hu, Z., Qiu, Y., Wang, H., & Liu, Y. F. (2014, March). A new model for designing multi-hole multi-permeability nonlinear LTCC inductors. In *Applied Power Electronics Conference and Exposition (APEC), 2014 Twenty-Ninth Annual IEEE* (pp. 757-762). IEEE.

[18] Wang, L., Hu, Z., Liu, Y. F., Pei, Y., & Yang, X. (2013). Multi-permeability Inductors for Increasing the Inductance and Improving the Efficiency of High-Frequency DC/DC Converters. *Power Electronics, IEEE Transactions on*, *28*(9), 4402-4413.

[19] Thermal Equivalent Circuit Models. *Infienon Technology AG, Application Note–May 2008.*

[20] Hirohata, K., Hisano, K., Mukai, M., Aoki, H., Takubo, C., Kawakami, T., & Pecht, M. G. (2010). Coupled thermal-stress analysis for FC-BGA packaging reliability design. *Components and Packaging Technologies, IEEE Transactions on*, *33* (2), 347-358.

[21] Yamada, Y., Yu, Q., Takahashi, T., & Takagi, Y. (2012, December). Study on thermal design due to downsizing of power module using coupled electrical-thermal-mechanical analysis. In*Electronic Materials and Packaging (EMAP), 2012 14th International Conference on* (pp. 1-7). IEEE.

[22] JEDEC standard: Jesd 51 " Methodology for the thermal measurement of component packages " , JEDEC solid state technology association.